University of Padova

Department of Physics "Galileo Galilei"

Bachelor Thesis in Physics

Hidden Markov Models for dimensionality reduction of neural activity

Hidden Markov Model per la riduzione dimensionale dell'attività neurale

Supervisor
Professor Samir Suweis
University of Padova

Co-supervisor
Dottor Giacomo Barzon
University of Padova

Candidate
Veronica Bedin

Student ID
1142199

Academic Year
2021-2022

Abstract

Recently, Hidden Markov Models (HMM) have been used to reduce the dimensionality of complex and high-dimensional data. In particular, it is known that neural activity recorded through electroencephalogram (EEG) displays low-dimensional global patterns of coordinated activity, termed "microstates". In this thesis we will first review the framework of HMM to then apply it on EEG data recorded from healthy subjects on 64 channels at rest (and during task). Finally, we will characterize the statistics on the low dimensional space, such as the average duration, the frequency of occurrence and the transition probabilities.

Recentemente, gli Hidden Markov Models (HMM) sono stati usati per ridurre le dimensioni di dati complessi e ad alta dimensionalità. In particolare, è noto che l'attività neurale registrata tramite elettroencefalogramma (EEG) presenta pattern globali di attività coordinate a bassa dimensionalità, chiamati "microstati". In questa tesi esamineremo prima il framework degli HMM per poi applicarlo ai dati EEG registrati in soggetti sani su 64 canali a riposo (e durante lo svolgimento di un compito). Infine, caratterizzeremo la statistica dello spazio a bassa dimensionalità, come la durata media, la frequenza di occorrenza e le probabilità di transizione.

Contents

1 Introduction

Neural activity comprises networks of individual neurons that perform sensory, cognitive, and motor functions, or perform non-trivial dynamics even when the brain is at its resting state. Neural population dynamics expresses how the activity of the neural population evolves through time and lives in principle in a high dimensional space (one dimension per neuron considered). However, in recent years, evidence is mounting that both spontaneous [1] and during task [2] neural activity is low-dimensional. This implies that the high dimensional neural activity in the empirical data can be described by clusters living in lower dimensional spaces [3]. Inferring such clusters is a complex unsupervised task, and typically can be done by use of machine learning algorithms.
In neuroscience, these techniques are applied both to animal [4, 5] and human [6] data, obtained by different techniques (e.g., local field potential and imaging, respectively). For instance, with magnetic resonance (MRI) data we are able to observe resting state networks [6]. These are macroscopic regions, co-activating in a synchronous way, even those that are structurally distant to each other.

Another widespread technique to study neural activity in humans is through electroencephalography signals (EEG). EEG enables the identification of finite numbers of brain maps representing simultaneous activation states of different parts of the brain, called microstates. They are stable for $100 - 200$ ms [7], with nearly simultaneous exchanges between one map at time t and another at time $t + 1$ and are typically found through clustering algorithms (e.g. k-means, hierarchical).

However these algorithms are "black boxes" and based on the minimization of high dimensional distance among data-points.

Recently, an alternative way to find microstates has been proposed, based on a family of stochastic process called Hidden Markov Models (HMM).
In this work we aim to study these microstates applying the HMM method to EEG data.

In *Chapter 2* we will give an overview of the mathematics behind HMMs, with a particular focus on the Gaussian kind. We will also introduce the Expectation Maximization method

(EM) to infer the hidden parameters of our HMM.

In *Chapter 3*, we will apply the theoretic framework of *Chapter 2* to our problem of study . We will manipulate our EEG data to infer the microstates of our system by reinterpreting our data as signals of a HMM. Finally, we will consider their importance in the study of brain activation states and their link to neuropsychological diseases.

In *Chapter 4*, all the data manipulation and experimental results will be presented. The results will provide a reference for the properties of the microstates that we expect to find in a healthy subject at rest.

2

Mathematical Introduction

2.1 Hidden Markov Models

A Markov chain is a stochastic process described by the sequence of successive states $Z = (Z_n)$ with $n = 0, 1, 2, \ldots$ in which the value z of Z_n at time n only depends on the value of Z_{n-1} at time $n - 1$. This property is called memorylessness, or Markov property. In mathematical terms:

$$p\left(Z_n | Z_{n-1}, Z_{n-2}, \ldots, Z_0\right) = p\left(Z_n | Z_{n-1}\right), \tag{2.1}$$

where p describes the probability distribution of the random variable Z_n at step n conditioned to the previous history, that because of the Markov property, is simply the state at the previous time step Z_{n-1}.

Whenever the process is in state z_i at time n, there is a fixed probability, P_{ij} (one-step transition probability), that it will be in state z_j at time $n + 1$:

$$P_{ij} = P\left(Z_{n+1} = z_j | Z_n = z_i\right) \tag{2.2}$$

Since probabilities are non-negative, and since the process must move from one state to another, we impose:

$$P_{ij} \geq 0 \quad i, j \geq 0 \quad \sum_{j=0}^{\infty} P_{ij} = 1 \quad i = 0, 1, \ldots \tag{2.3}$$

A Hidden Markov Model (HMM) is a Markov chain in which the states are not directly observable. More precisely, the chain has a certain number of states that evolve as a Markov chain. Every state generates with a certain probability distribution a signal x from an either continuous or discrete set, only depending on the state. The signal is observable but the state is not. A depiction of the process is shown in Figure 2.1:

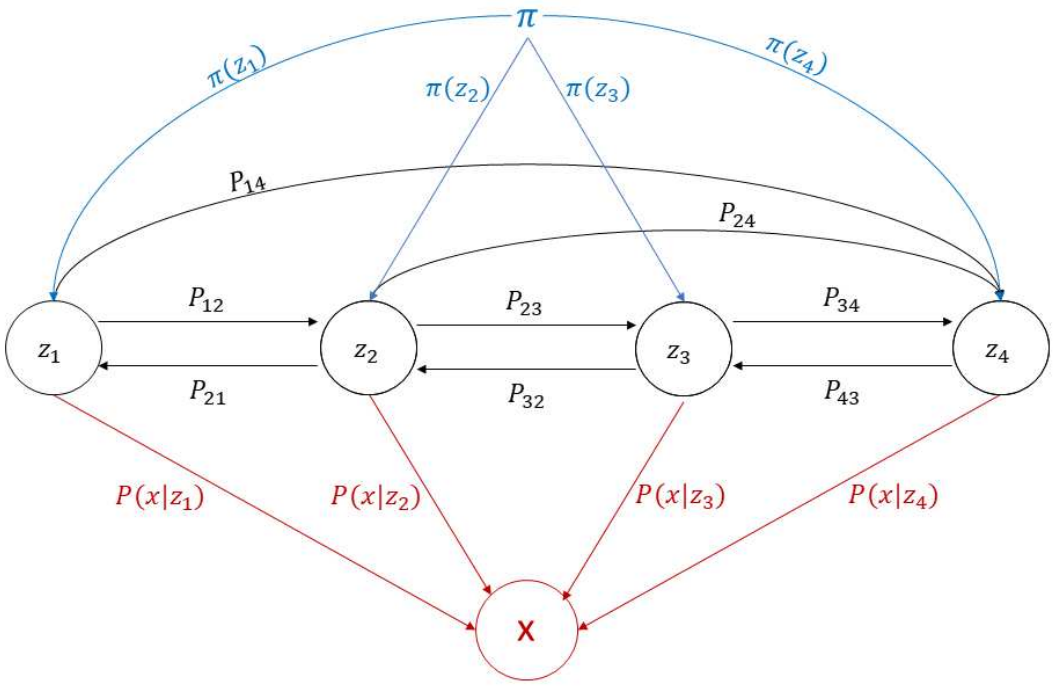

Figure 2.1: A representation of a HMM with $K = 4$ hidden microstates. In *black*: z_i are the hidden states that form the Markov chain and the P_{ij} are the probabilities of moving from state i to state j. Only some of them are represented in this figure. In *red*: x is the observed signal at time t (it could be continuous or discrete) and $P(x|z_i)$ are the probabilities of observing signal x at given state z_i. In *blue*: π is the initial probability distribution while $\pi(z_i)$ is the probability that the HMM will start at microstate i.

A HMM is completely determined by its three parameters $(\pi, \mathbf{A}, \mathbf{B})$.
Parameter $\mathbf{A}$ is defined as the *transition probability matrix*, a matrix in which each cell a_{ji} expresses the probability P_{ij} to move from the microstate i to the microstate j via subsequent time steps.
Parameter $\mathbf{B}$ is defined as the *emission probability* $P(x|z)$, which is the conditional probability to observe a signal x if the hidden state is z. This probability can either be discrete (e.g. a Bernoulli) or continuous (e.g. a Gaussian or a t-Student).
The last parameter, π, is the initial probability distribution, associated to probability of being in the different states at time $n = 0$.

As states cannot be observed directly, our goal is to get information on them by observing the sequence of signals $X = (X_n)$.

The signals in our study are multivariate observation sequences, that is at time t we have a signal $X_t = \mathbf{x} = (x^{(0)}, x^{(1)}, ..., x^{(N)})$, with N being the dimension of our signal. Hence, the emission probabilities are multivariate Gaussian densities and **B** represents the *emission probability distributions*, i.e. **B** is a set of continuous multivariate probability distributions (one for each state z), each dictating the probability of the HMM to generate a signal **x**, given the current state z.
The probability distributions will be in the form:

$$P(\mathbf{x}|z) = \mathcal{N}_D(\boldsymbol{\mu}_z, \boldsymbol{\Sigma}_z) \tag{2.4}$$

which means that every hidden state z will emit a multivariate signal with D-dimensional mean $\boldsymbol{\mu}_z$ and DxD covariance matrix $\boldsymbol{\Sigma}_z$.

2.2 Expectation-Maximization algorithm

To learn the parameters of the HMM, namely $(\pi, \mathbf{A}, \mathbf{B})$, one can exploit the Expectation Maximization algorithm. Given a statistical model that depends on hidden variables, the EM algorithm is an iterative method to find maximum likelihood local estimates of the parameters of the model so that the HMM generate a signal that match the empirical signal X.
Let $l(\theta|X, Z)$ be the complete-data log likelihood, where X represents the complete signal dataset, Z represent the corresponding hidden state sequence and θ is the unknown vector of parameters that we want to find (in our study case, $\theta = (\pi, \mathbf{A}, \mathbf{B})$).
The iteration of the EM algorithm alternates two steps:

- Expectation (E): estimates the expected value of $l(\theta|X, Z)$, at given X, and the current estimate on parameters θ_{old}. We define

$$Q := E[l(\theta|X, Z)|X, \theta_{old}] \tag{2.5}$$

$$= \int l(\theta|X, z)p(z|X, \theta_{old})dz \tag{2.6}$$

  with $p(z|X, \theta_{old})$ being the conditional density of z given the signals X and Θ_{old} is the old vector parameter.

- Maximization (M): maximizes equation 2.5 over θ. We set:

$$\theta_{new} := \max_{\theta} Q(\theta|\theta_{old}) \tag{2.7}$$

and then $\theta_{old} = \theta_{new}$

These estimates of the parameters are used to determine the distribution of the latent variables at the next Expectation step. The algorithm stops after a fixed number of iterations or when θ converges.

The hidden variables $\mathbf{Z}$ form the latent space that is the actual low dimensional space where we can embed the high dimensional signal $\mathbf{X}$. In the next chapter we are going to apply this HMM method to EEG data.

3

EEG microstates

The Hidden Markov Models will be useful to study the resting state activity of the human brain, measured via multichannel electroencephalography (EEG). What we are looking for are the electrical microstates of the brain, defined as "global patterns of scalp potential topographies recorded using multichannel EEG arrays that dynamically vary over time in an organized manner" [8]. EEG consists in the recording of the electric potential associated to the spontaneous electrical activity of the brain by means of a set of N electrodes. Each one of them is collecting data from a different region of the scalp. The observation of all the signals at once is characterized by oscillations in time that are not completely random. Instead, it can be observed a repetition of global patterns that correspond to the activation of different parts of the brain, visualized via scalp topography maps. The scalp topographies, from now on called *maps*, typically remain stable for a time period of 60-120 ms [9], then change abruptly to another map. Each one of these map is correspondent to what is called a microstate and reflects the momentary state of global neural activity, while the switching between microstates reflects a reorganization of it over time. The sequence of microstates alternating over time can be described by means of a HMM where the signals are given by a manipulation of the EEG data.

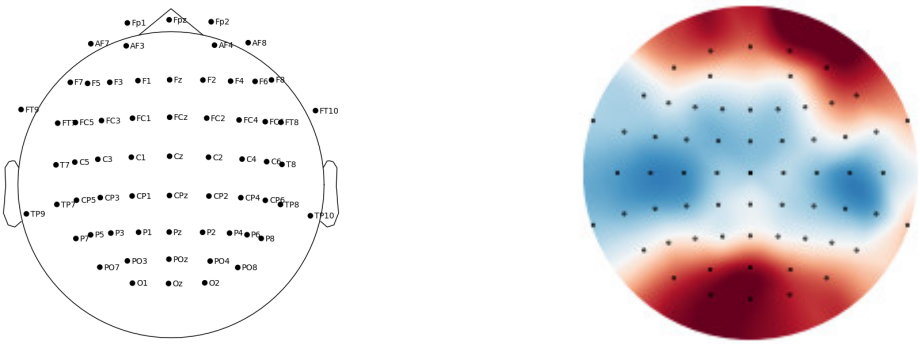

(a) Channels position

(b) Scalp topography map

Figure 3.1: Panel **(a)** is an example, taken from our data, of a 2-D representation of the scalp with the points corresponding to the position of the electrodes in it. Panel **(b)** represents one of the possible topographical maps, with the different colors representing a different value of the voltage.

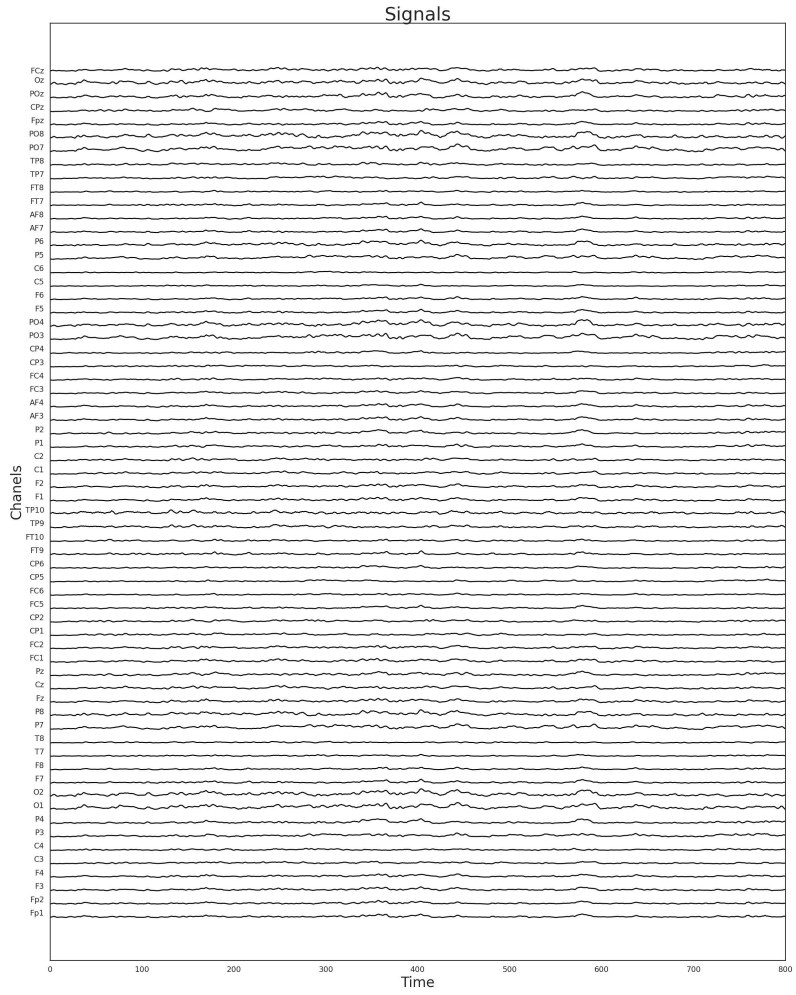

Figure 3.2: An example, taken from our data, of a EEG signal, with oscillation of voltage for the 64 different channels.

3.1 Problem modelization

3.1.1 Data manipulation

First of all, the signal is manipulated by calculating what is called the Global Field Power (GFP) at each instant of time t, correspondent to the spatial standard deviation of the signal, defined as:

$$GFP(t) = \sqrt{\frac{\sum_{n=1}^{N}(V_n(t) - \hat{V}(t))^2}{N}}$$

with V_n being the potential at the electrode n and $\hat{V}$ the mean of the potential over the N electrodes.

What we are interested in are the peaks of the GFP (its local maxima), that represent the instants of highest topographical signal-to-noise ratio. In microstate analysis, the local maxima of the GFP are interpreted as discrete states of the EEG and to each one of them corresponds a different map. A clustering algorithm is then employed to group similar maps into K different clusters. Each cluster is one of the actual *microstates* and is associated to a representative map.

The evolution of the GFP is then reinterpreted as a sequence of these microstates, with each GFP peak mapped to the microstate that it best correlates to.

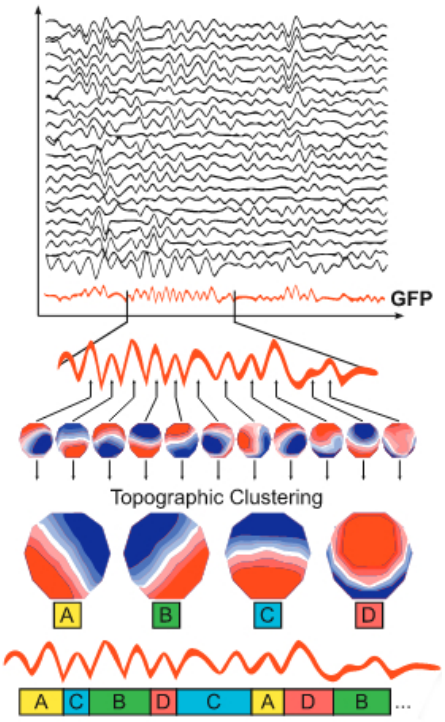

Figure 3.3: An example of microstate clustering and analysis. Multichannel EEG signal is used to calculate the GFP curve (drawn in red). To each maximum of the GFP is associated a topographical map and a microstate. In this case 4 maps are enough to explain most of the signal [10] and each one is labeled with a name: A,B,C or D. After that, to the maxima of the GFP signal are assigned the microstates that they best correlate to. [11]

Different values of K explain a different value of the global explained variance (GEV), which measures the percentage of data variance (i. e. the sum of the GFP values calculated at each time step) explained by a given set of microstates [9]. However, even if there is a large number of topographical maps that can explain the data, most ($58 - 84\%$ [9]) of the signal is usually de-

scribed by just a few of them. Indeed, the value of K has commonly been identified in literature to be of a few units, typically in the range $2 - 15$ [9, 7].

The choice of K can be made according to a variety of criteria (e.g. Marriot's criterion, simmetrized distance, hierarchical clustering) and must be performed such to reach a compromise between the needs for specificity, that would give a higher value of GEV and that typically benefits from a higher number of maps, and generalizability, so that the intrinsic differences between individuals will not tamper our results.

3.1.2 Application of HMM

To infer the sequence of microstates over time from our EEG signals, we describe our data by means of a Hidden Markov Model. In this particular case, the hidden microstates assume their values in a discrete and finite set $\{z_0, ..., z_{K-1}\}$, while the signal X corresponds to the sequence of the discrete peaks of the GFP.

The emission probability for state z_t is described by an N-dimensional Gaussian distribution — with N being the number of EEG channels — of means $\boldsymbol{\mu}_k$ and covariance matrix $\boldsymbol{\Sigma}_k$:

$$P(\mathbf{x}|z) = \mathcal{N}_N(\boldsymbol{\mu}_z, \boldsymbol{\Sigma}_z) \tag{3.1}$$

Once the model has been formalized, via the Expectation Maximization algorithm we can infer the emission and transition probabilities from the data.

Via the transition probabilities, the average voltage of the signal associated to a microstate can be inferred and from a combination of that information and the transition probabilities, the hidden sequence of microstates is reconstructed.

Finally, to understand the activity of the brain at rest or during specific tasks, from the sequence of microstates one would infer the following parameters:

- *Mean lifetime*: the average time during which a microstate is stable;
- *Fractional occupancy*: the fraction of time during which a microstate is active compared to the total data acquisition time;
- *Occupancy probability*: the probability for a microstate to be active regardless of its duration;
- *Transition probability matrix*: the matrix in which each entry is the transition probability between microstates.

3.2 Microstate study applications

In previous works [12, 13, 14], studying the brain activity microstates allowed to understand that the brain at rest is not inactive, but active in an organized way, so that it is always ready to process different stimuli.

It has been proven that transition probabilities are non-random [15, 16], that in people with schizophrenia they are altered [15, 17] and that in patients with dementia the sequence of microstates is indistinguishable from a random process [18]. Therefore, "the time-course of the information flow between different brain states is crucial for ensuring the perception of incoming stimuli, proper cognitive processing and adequate action in a conscious manner" [9]. The EEG microstate sequence can be observed at different time scales and at each of one they reveal the same information (*scale free property*). It has been observed that variations in lifetime duration of specific microstates have been associated to several neuropsychiatric diseases, indicating that failure of the scale-free property and changes in microstate lifetimes impact on neurological and psychiatric conditions.

Different studies focused on schizophrenia [19, 20, 15, 18], both in medicated and unmedicated patients, as well in patients with hallucinations and in people at risk of developing the disease. These studies used K=4 and the microstates were named A, B, C and D. It has been observed, in patients with schizophrenia, that microstate C appears more frequently and that microstates B,D mean lifetimes are shorter. Based on the studies of microstates in altered states of consciousness (e.g. hypnosis, meditation, sleep), it seems that there is a functionally relevant balance between states C and D and that "a preponderance of microstate C may result in a progressive detachment of mental states from environment input" ([9]).

Other applications of microstate analysis were used for other diseases e.g. narcolepsy, dementia, panic disorder, head injury, diplegia, stroke and multiple sclerosis. In most of these cases a decrease in duration of C and changes in A and B have been observed, while the balance between C and D seems to be conserved. This suggests that variations of C and D are specific to schizophrenia.

4

Data analysis

4.1 Experiment setup and data preprocess

The data used in our experiment were collected from 44 healthy subjects at rest, via a 64 channel electrode cap, at a frequency of 500 *Hz* and filtered through a bandpass filter with range $1 - 100$ *Hz*.
Afterwards, the data were cleaned via artifact removal algorithms, used to remove the main sources of interference in our EEG data, specifically ocular, muscular and cardiac artifacts.
Additional preprocessing done on every subject data:

1. A $4 - 30$ *Hz* bandpass filter was applied;
2. The signal was downsampled, meaning that the sampling rate of the signal was reduced, at 200 *Hz*;
3. The amplitude envelope was calculated via the Hilbert transform;
4. The signal was downsampled again at 40 *Hz* with a sliding window of 100 *ms* (20 timestep) with 75% overlap;
5. Standardization was applied: from the signal it was subtracted the average and afterward it was divided by the standard deviation;
6. The data of every subject was concatenated in a single array;
7. The dataset dimensionality was reduced via Principal Component Analysys (PCA) from $N = 64$, the number of electrodes, to $M = 10$. The value of N of the previous chapters will be from now on $M = 10$, and every dimension $j \in (0, \dots, M - 1)$ will be referred to as *channel j*;
8. The whitening transformation was applied.

PCA is a dimensionality-reduction algorithm, used to infer from large set of variables a smaller set that still contains most of the previous information. Some of the variables belonging

to the set obtained by PCA could be correlated with each other then, via whitening transformation, we obtain a set of uncorrelated variables each of variance 1.

All the preprocessing was done by Dr. Barzon of LIph LAB.

The data that we obtain after the preprocess was a 10 dimensional array, lasting 440000 timesteps which corresponds to more or less 3 *hours*.

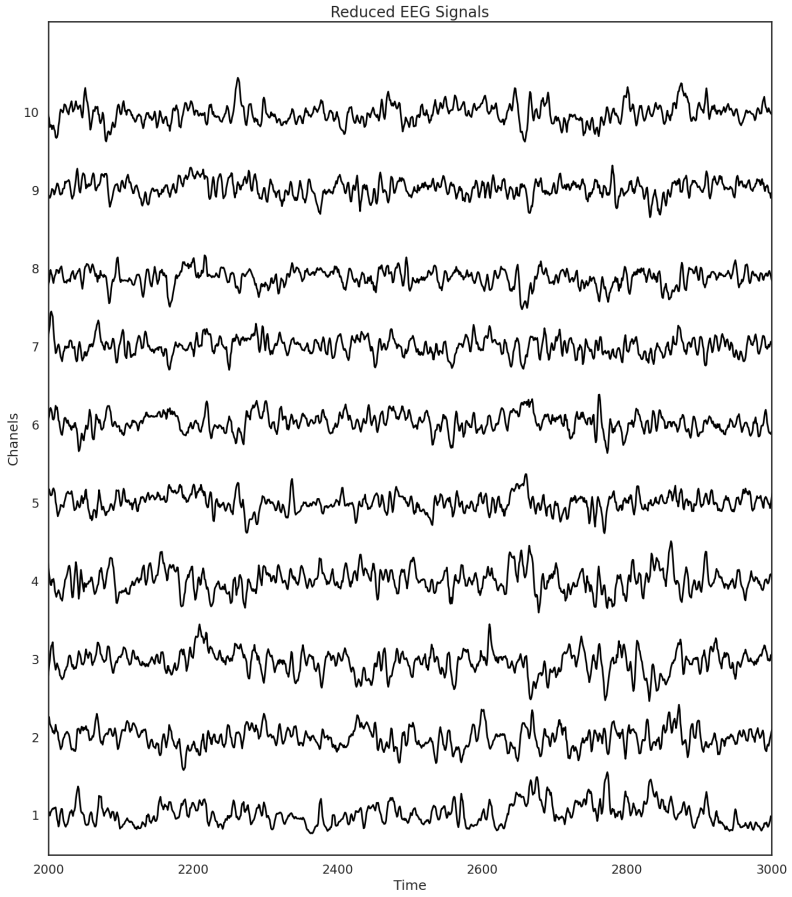

Figure 4.1: An example of the data obtained after the preprocess. Only a part of it is shown to clearly see the signal

4.2 Data analysis

The dataset obtained after the preprocess (a fraction of which is shown in Figure 4.1), is used as the signal in our HMM. K, the number of microstates, was chosen as equal to 6, following a choice made in different studies (e.g. [7]). The microstates are referred to as $0, 1, 2, 3, 4, 5$. After fixing K, we implemented the EM algorithm, from which we inferred the mean voltage

(Table 4.1) and the covariance matrix (Figure 4.3) for each microstate. The algorithm was run for 50 iterations and we see in Figure 4.2 that it converges after $10-15$ iterations. In Figure 4.2 the log probability is another way of calling the log-likelihood $l(\theta|X,Z)$, introduced in chapter 2. The results are shown below:

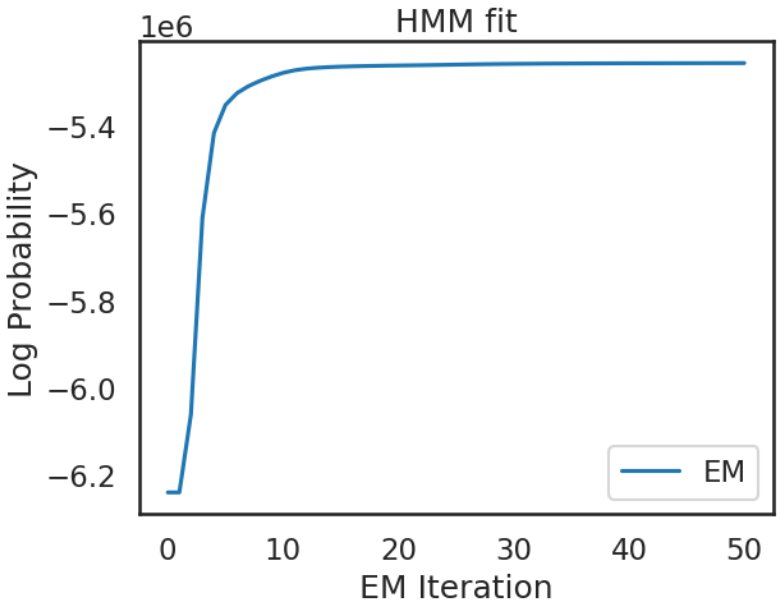

Figure 4.2: Plot of the log probability versus the step in the EM iteration, created to visualize the converge of the EM algorithm, with the number of maximum iterations set at 50. We see that it converges after the first $10-15$ iterations.

Channel	State 0	State 1	State 2	State 3	State 4	State 5
1	-0.2 ± 0.7	2 ± 1	0.1 ± 0.8	0.3 ± 0.8	0.0 ± 0.8	-0.9 ± 0.6
2	0.2 ± 0.9	1 ± 1	-0.3 ± 0.9	-0.6 ± 0.9	0.6 ± 0.9	-0.2 ± 0.7
3	0.3 ± 0.9	0 ± 1	0.3 ± 0.9	-0.9 ± 0.8	0.3 ± 0.9	-0.1 ± 0.7
4	0.6 ± 0.8	0 ± 1	-0.7 ± 0.9	0.2 ± 0.9	0.0 ± 0.9	-0.1 ± 0.7
5	0.2 ± 0.9	0 ± 1	0 ± 1	0.0 ± 0.8	0 ± 1	-0.1 ± 0.7
6	-0.1 ± 0.9	0 ± 1	-0.2 ± 0.9	0.2 ± 0.9	0 ± 1	-0.1 ± 0.7
7	-0.7 ± 0.8	0 ± 1	-0.2 ± 0.9	0.1 ± 0.8	0.8 ± 0.9	0.1 ± 0.7
8	0.4 ± 0.9	0 ± 1	0.2 ± 0.9	0.0 ± 0.9	-0.2 ± 0.9	-0.1 ± 0.7
9	-0.1 ± 0.9	0 ± 1	0.2 ± 0.9	0 ± 1	0 ± 1	0.0 ± 0.7
10	0.0 ± 0.9	0 ± 1	-0.4 ± 0.9	0.2 ± 0.9	0 ± 1	-0.1 ± 0.7

Table 4.1: Mean voltage and standard deviation associated to each state and each channel. Each entry is expressed in mV

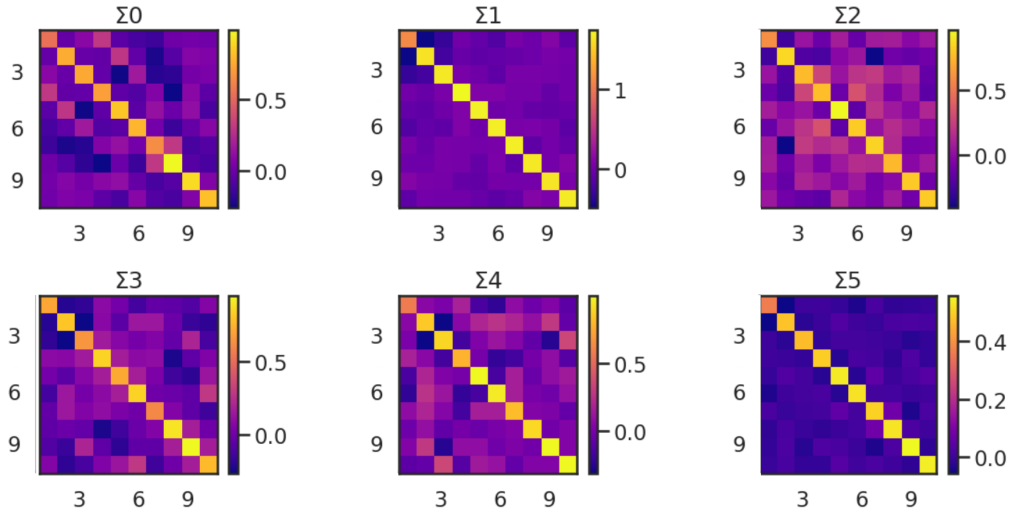

Figure 4.3: The covariance matrices, one for every microstate. Each entry is a different channel. Colorbar is in mV^2

Another thing we can infer through the EM algorithm is the transition probability matrix, also known as the parameter $\mathbf{A}$ of our HMM.

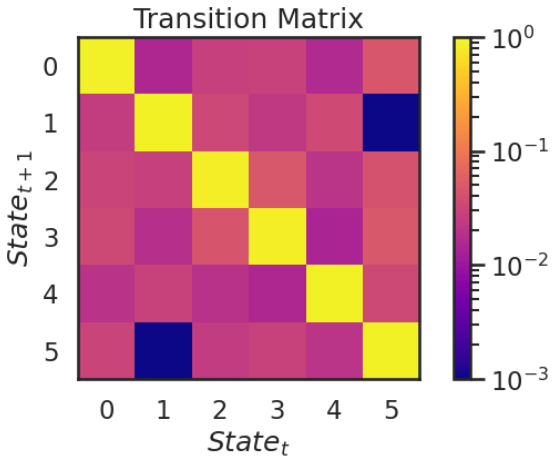

Figure 4.4: Plot showing the log transition probability matrix between state at time t and state at time $t+1$. It's clearly visible that a state almost always evolves into itself, and if we tried to compute the normal transition probability matrix we would just see the principal diagonal being different from all the other entries. For a better visualization of the processes, we need to compute the log matrix

From these results, we can finally infer the sequence of hidden microstates of the whole dataset.

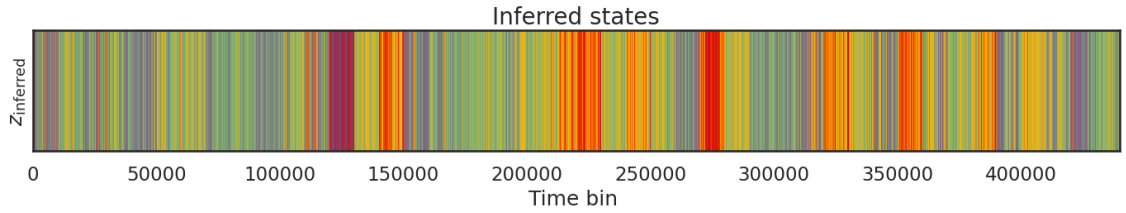

Figure 4.5: Plot of the sequence of microstates. Each color corresponds to a different microstate.

We then calculate some typical parameters of microstate analysis: the *mean lifetime* in Figure 4.6, the *occupancy probability* in Figure 4.7 and the *fractional occupancy* in Figure 4.8.

Noting the presence of values in our dataset that are far from the mean, we remove outliers by considering as such the numbers that are more than 1.5 times the interquartile range (IQR) away from the mean. We define quartiles as those values that divide the data into four portions, each containing approximately the same amount of points. 25% of the data is below the first quartile and 75% of the data is below the third quartile. The IQR is a quantity defined as the difference between the first and third quartiles. Thus, within the IQR there will be 50%of the data, those that we consider most relevant to our statistics.

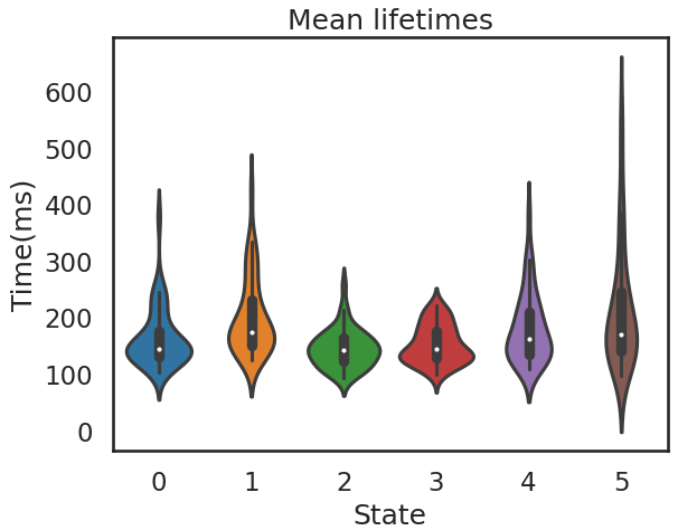

Figure 4.6: Violinplot showing the microstate mean lifetime. The white dot indicates the median, the thick black line is the IQR, the thin black line is 1.5∗IQR and the colored shapes the probability density of the variable, simmetrically mirrored along the y axis.

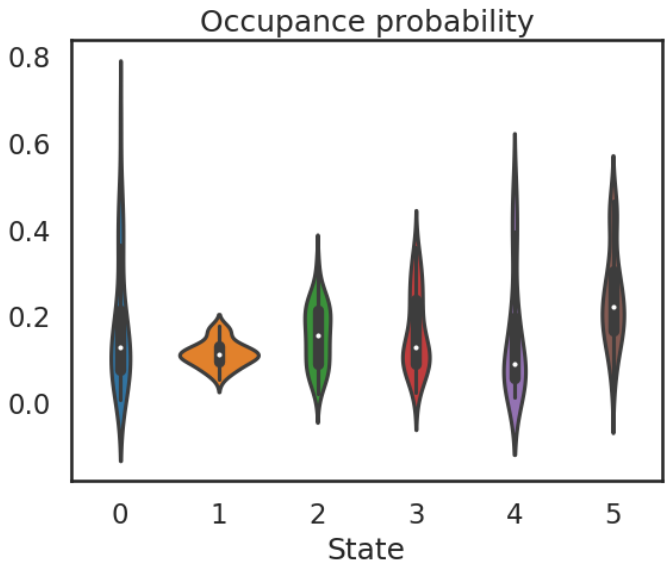

Figure 4.7: The plot of the occupancy probability of every microstate. The data is represented as before.

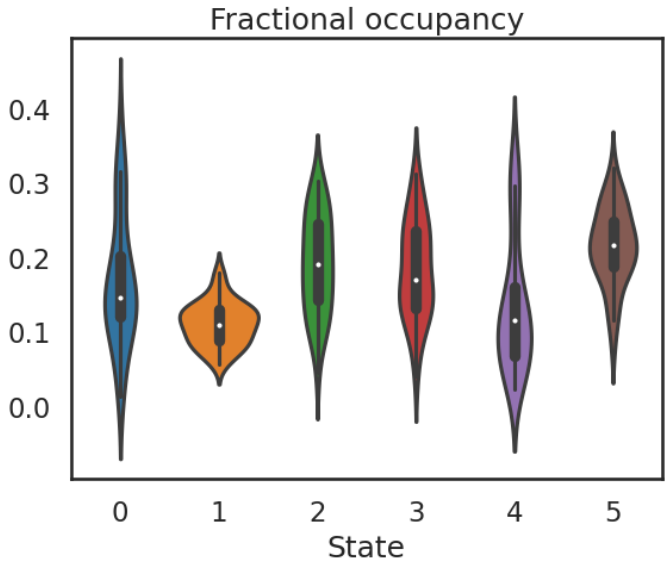

Figure 4.8: The plot of the fractional occupancy of every microstate.The data is represented as before.

Finally, we infer from the sequence in Figure 4.5 the activation and deactivation array of each state over time, meaning an array that is 1 if the microstate at that time step t is active, 0 otherwise. Once for every microstate, every time step of its activation/deactivation array will be

correlated to the correspondent time step in each one of the 64 channel of the original dataset, obtaining at the end $K = 6$ arrays of correlation coefficients, shown below.

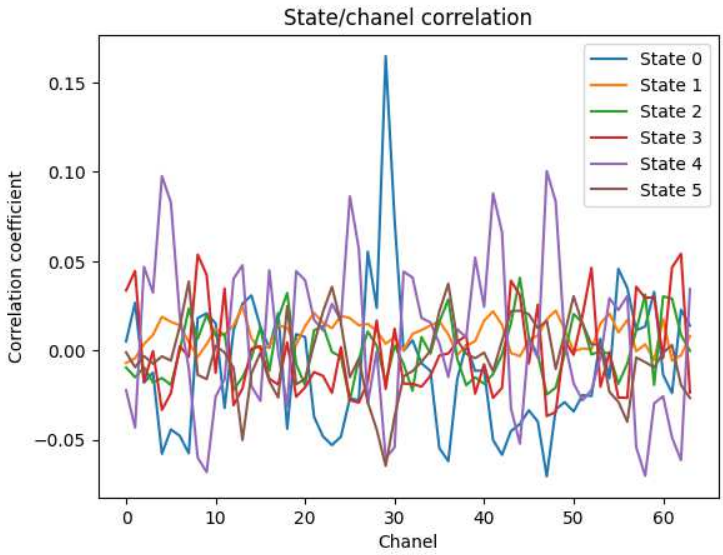

Figure 4.9: The plot of the 6 correlation coefficients with respect to the channel.

This lets us know which electrodes, and consequently which parts of the brain, are active during the activation of a certain microstate, and we infer the topographical maps in Figure 4.10.

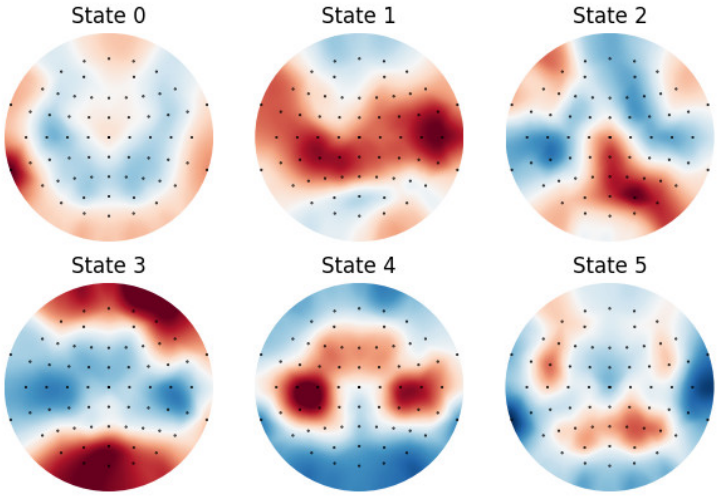

Figure 4.10: The topographical maps associated to each microstate. Red is associated with a $+1$ correlation coefficient between the activation and the signal arrays, meaning an activation of that part of the brain in that microstate, while blue is associated with -1 and a deactivation of that part of the brain.

5 Discussion

First of all, we proved the EM algorithm used to infer the HMM parameters **A** and **B**, respectively the transition probability matrix and the emission probabilities, converges very quickly, after the first $10 - 15$ iterations, as can be seen in Figure 4.2.
We then found via the transition probability matrix that if a microstate is i at time t, it will remain i at time $t + 1$ with a probability close to 1. This is explained by the fact that for most of the time the microstates are stable and that the switching between two of them is practically instantaneous. Another interesting fact we can infer from the matrix is that State 1 almost never evolves into State 5, and vice versa.

The inferred mean lifetimes and fractional occupancies are reported below (mean $\pm$ standard deviation):

Microstate	Mean lifetimes (ms)	Fractional occupancies (%)
0	160 ± 70	17 ± 9
1	200 ± 70	11 ± 3
2	150 ± 70	19 ± 7
3	150 ± 70	18 ± 6
4	180 ± 70	13 ± 9
5	210 ± 70	21 ± 5

Table 5.1: Mean lifetimes and fractional occupancies with STD of each microstate.

Comparing the results obtained by *Coquelet et al.* [7] where 6 microstates were employed as well, it can be appreciated that the average durations of each microstate are in the same $130 - 230$ ms time range and that the fractional occupancies are also compatible, even if it is not possible to map $1 : 1$ their microstates with those obtained from our dataset.

	EEG HMM	
	Mean lifetimes (ms)	Fractional occupancies (%)
State 1_{EEG}	136 ± 19	17 ± 3.7
State 2_{EEG}	145 ± 39	13.3 ± 4.5
State 3_{EEG}	204 ± 70	8.4 ± 1.4
State 4_{EEG}	226 ± 109	22.4 ± 9
State 5_{EEG}	137 ± 20	14.6 ± 4.7
State 6_{EEG}	141 ± 23	24.3 ± 6.2

Figure 5.1: Results for mean lifetimes and fractional occupancies for each microstates from *Coquelet et al.* [7], reported with their standard deviation. Here the microstates have a different label but K is still equal to 6 [7]

Finally, a comparison can be made between the activation areas highlighted by our microstates (red in Figure 4.10) and the functional areas of the cerebral cortex, shown in Figure 5.2.

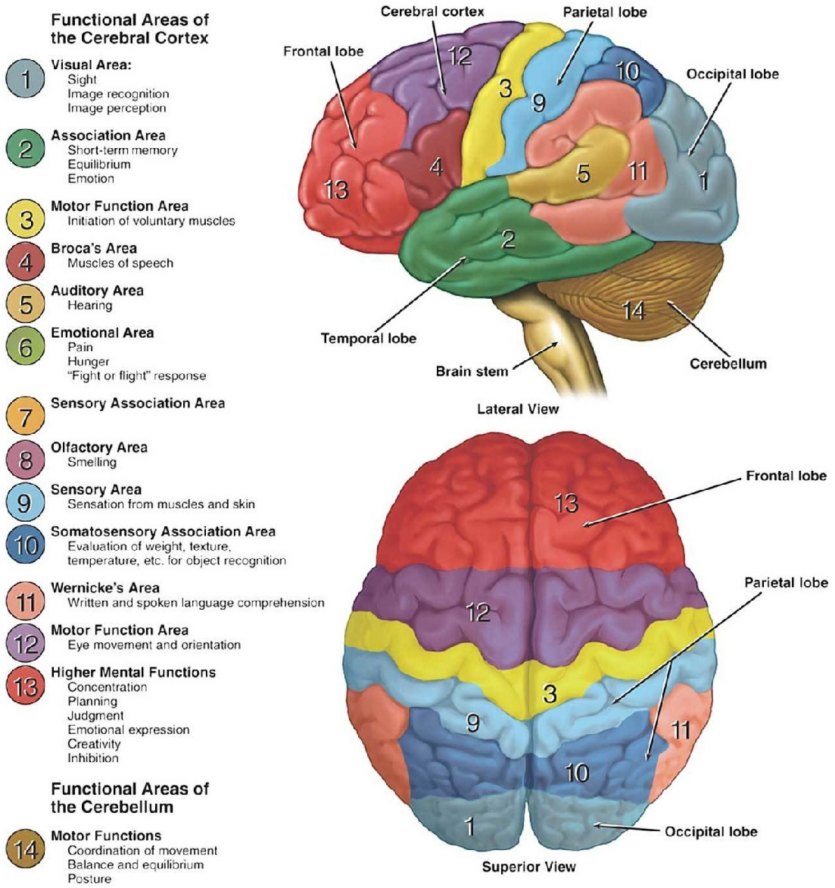

Figure 5.2: A representation of the functional areas of the cerebral cortex, from the side and from above. [21]

The microstates which have brain activation areas clearly correspondent to functional areas of the cerebral cortex are $S0, S1$ and $S3$. In particular, the functional areas implicated in these states are (the numbers corresponds to the ones in Figure 5.2):

- *Visual area* (1): corresponds to the occipital lobe and is responsible of sight, image recognition and image perception;
- *Association area* (2): corresponds to the temporal lobe and is responsible for short term memory, equilibrium and emotion;
- *Motor function area* (3): located between the parietal lobe and the cerebral cortex, responsible for the initiation of voluntary muscles;
- *Sensory area* (9) : located in the parietal lobe, it's responsible for encoding the sensations from muscles and the skin;
- *Somatosensory association area* (10): it's in the parietal lobe and it's responsible for the evaluation of parameters (e.g. weight, texture, temperature) for object recognition;
- *Motor function area* (12): corresponds to the cerebral cortex and is responsible for eye movement and orientation;
- *Higher mental function area* (13): it corresponds to the frontal lobe and is responsible of things as concentration, planning, creativity, inhibition, judgment and emotion expression.

Area \ State	0	1	3
Visual(1)	⋆		⋆
Association(2)	⋆	⋆	
Motor function (3)		⋆	
Sensory (9)		⋆	
Somatosensory association (10)			⋆
Motor function (12)		⋆	
Higher mental function (13)			⋆

Table 5.2: Activated functional areas (indicated by ⋆) for microstates $S0, S1, S3$

6 Conclusion

The goal of this research was to study the brain activity of healthy subjects at rest. We applied the HMM and an EM algorithm to reduce the dimensionality of a 64-channel EEG. By doing this we showed that the signal displays low-dimensional global patterns of coordinated activity, termed *microstates*.

After fixing the number of microstates at $K = 6$, we inferred from our data the statistics of the low dimensional space. In particular, we inferred the average duration, the frequency of occurrence, the occupation probability of each microstate, as well as the transition probability matrix.

Finally, we visualized the topographical maps of each microstate and correlated some of them to the different functional areas of the cerebral cortex.
Our research proved that different areas of the brain, even if distant and not connected, activate at the same time for short periods of time. This leads us to conclude that the brain, even when at rest, is always ready to react to different stimuli.

In future work, the model could be improved by inferring the number of microstates through Bayesian data-driven methods, or according to the procedures analyzed by *Pohle et al.* in [22]. In fact, in our case we just set the number of microstates based on previous literature, without further explorations.

Despite these limitations, we were able to provide a reference for the microstates and their properties that we expect in healthy subjects at rest. In future work, these could be used as biomarkers to distinguish healthy subjects from those with neuropsychiatric diseases, or to distinguish subjects at rest from those who are performing tasks.

References

[1] S. Mehrkanoon, M. Breakspear, and T. W. Boonstra, "Low-dimensional dynamics of resting-state cortical activity," *Brain topography*, vol. 27, no. 3, pp. 338–352, 2014.

[2] J. A. Gallego, M. G. Perich, S. N. Naufel, C. Ethier, S. A. Solla, and L. E. Miller, "Cortical population activity within a preserved neural manifold underlies multiple motor behaviors," *Nature communications*, vol. 9, no. 1, pp. 1–13, 2018.

[3] Pezzulo et. al, "The secret life of predictive brains: what's spontaneous activity for?" 2021.

[4] Celletti and Villa , "Low-dimensional chaotic attractors in the rat brain," 1996.

[5] Gallego et al., "Neural manifolds for the control of movement," 2017.

[6] Seitzman et al., "The state of resting state networks," 2019.

[7] Coquelet et al., "Microstates and power envelope hidden markov modeling probe bursting brain activity at different timescales," 2022.

[8] Lehmann et al., "Eeg alpha map series: brain micro-states by space-oriented adaptive segmentation."

[9] Michel and Koenig, "Eeg microstates as a tool for studying the temporal dynamics of whole-brain neuronal networks: A review," 2018.

[10] Lehmann et al., *Electroencephalogr. Clin. Neurophysiol.*
EEG alpha map series: brain micro-states by space-oriented adaptive segmentation, 1987.

[11] Khanna et al., "Microstates in resting-state eeg: Current status and future directions," 2014.

[12] Fox and Raichle, "Spontaneous fluctuations in brain activity observed with functional magnetic resonance imaging," 2007.

[13] Fox et al., "The human brain is intrinsically organized into dynamic, anticorrelated functional networks," 2005.

[14] Greicius et al., "Functional connectivity in the resting brain: a network analysis of the default mode hypothesis," 2003.

[15] Lehmann et al., "Eeg microstate duration and syntax in acute, medication-naive, first-episode schizophrenia: a multi-center study," 2005.

[16] Wackerman et al., "Adaptive segmentation of spontaneous eeg map series into spatially defined microstates," 1993.

[17] Tomescu et al., "Schizophrenia patients and 22q11.2 deletion syndrome adolescents at risk express the same deviant patterns of resting state eeg microstates: a candidate endophenotype of schizophrenia," 2015.

[18] Nishida et al., "Eeg microstates associated with salience and frontoparietal networks in frontotemporal dementia, schizophrenia and alzheimer's disease," 2013.

[19] Dierks , Strik et al., "Eeg-microstates in mild memory impairment and alzheimer's disease: possible association with disturbed information processing," 1997.

[20] Irisawa et al., "Increased omega complexity and decreased microstate duration in nonmedicated schizophrenic patients," 2006.

[21] Dana foundation, "Neuroanatomy: the basics."

[22] Pohle et al., "Selecting the number of states in hidden markov models: Pragmatic solutions illustrated using animal movemen," 2017.